

## Supplemental Methods



**Figure S1. Schematic of the CAR19 transposon cassette.** The pVAX1PB

CAR19h28TM41BBz transposon plasmid contains the following functional DNA sequences

making up the transposon cassette: the **hEF1alpha promoter** (GenBank HG530137.1,

FJ716125.1)<sup>1,2</sup>, the **CAR19h28TM41BBz chimeric antigen receptor** and the **SV40**

**polyadenylation signal**<sup>3-5</sup>. In addition, the functional sequences are flanked by **chicken β-globin**

**cHS4 insulators** intended to prevent the transgene altering expression of surrounding genes or

CAR transgene silencing<sup>6-9</sup>, which are in-turn flanked by the **transposon inverted repeats**

(GenBank HQ888845.1, EU257621.1, KF658273.1, AB779767.1, AB779766.1)<sup>10-12 13,14</sup>. IR=

inverted repeat, Ins= Insulator, EF1α= human elongation factor-1 alpha promoter,

CAR19h28TM41BBz= CD19-specific CAR transgene, SV40= simian virus late polyadenylation

*signal*.

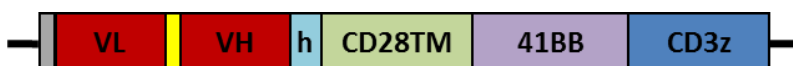


**Figure S2. Schematic of CAR19h28TM41BBz Transgene.** The CAR19h28TM41BBz

**transgene** is a second generation CAR consisting of the CD8 alpha chain leader peptide (amino

acids 1-21, UniProtKB reference P01782), a single chain variable fragment (scFv) derived from

the CD19-specific antibody, FMC63<sup>15,16</sup> containing a flexible (G4S)3 linker<sup>17,18</sup>. The scFv is

followed by a second (G4S)3 linker and an extracellular spacer consisting of the hinge domain of

the human IgG1 heavy chain (amino acids 99-110, UniProtKB reference P01857) with a C to P

amino acid substitution in the hinge domain at position 103 of the native protein. The spacer is followed by the transmembrane domain of the CD28 molecule (amino acids 153-179, UniProtKB reference P10747) and then the intracellular domains of 4-1BB (CD137- amino acids 214-255, UniProtKB reference Q07011) and CD3zeta (amino acids 52-164, UniProtKB reference P230963). Grey bar= CD8 alpha leader peptide sequence; VL= FMC63 antibody light chain variable region sequence; VH= FMC63 antibody heavy chain variable region sequence; h= IgG1 hinge; CD28TM= transmembrane domain of the CD28 co-stimulatory molecule; 41BB= intracellular domain of 4-1BB (CD137), CD3z= intracellular domain of CD3 zeta chain.

*Annotated Sequence of the pVAX1PB CAR19h28TM41BBz Plasmid*

5' IR 201-139 (c)

Insulator 377-608

EF1alpha Promoter 622-1167

CAR19 1194-2657

SV40 polyA 2779-2909

Insulator 3388-3158

3' IR 3663-3697

Kanamycin R 4271-5065

pUC ori 5364-6037

Non-coding

GACTCTTCGCGGCGCGCCTCGTTCATTCACGTTTTTTGAACCCGTGGAGGACGGGCAG  
ACTCGCGGTGCAAATGTGTTTTACAGCGTGATGGAGCAGATGAAGATGCTCGACAC  
GCTGCAGAACACGCAGCTAGATTA**CCCTAGAAAGATAATCATATTGTGACGTAC**  
**GTTAAAGATAATCATGTGTAAAATTGACGCATG**TGTTTTATCGGTCTGTATATCGA  
GGTTTTATTTATTAATTTGAATAGATATTAAGTTTTATTATTTACACTTACATACTA  
ATAATAAATTCAACAAACAATTTATTTATGTTTATTTATTTATTAACAAAAACAAAA  
ACTCAAAATTTCTTCTATAAAGTAACAAAACCTTTTAT**GAGGGACAGCCCCCCCCAA**  
**AGCCCCAGGGATGTAATTACGTCCCTCCCCCGCTAGGGGGCAGCAGCGAGCCGCC**  
**CGGGGCTCCGCTCCGGTCCGGCGCTCCCCCGCATCCCCGAGCCGGCAGCGTGCGG**  
**GGACAGCCCGGGCACGGGGAAGGTGGCACGGGATCGCTTTCCTCTGAACGCTTCTC**  
**GCTGCTCTTTGAGCCTGCAGACACCTGGGGGGATACGGGGAAAA**GGCCTCCACGGC  
CAAGGATCTGCGATCGCTCCGGTGCCCGTCAGTGGGCAGAGCGCACATCGCCACA  
GTCCCCGAGAAGTTGGGGGGAGGGGTCCGGCAATTGAACGGGTGCCTAGAGAAGGTG  
GCGCGGGGTAAACTGGGAAAGTGATGTCGTGTA**CTGGCTCCGCCTTTTTCCCGAGGG**  
TGGGGGAGAACCGTATATAAGTGCAGTAGTCGCCGTGAACGTTCTTTTTCGCAACGG  
GTTTGCCGCCAGAACACAGCTGAAGCTTCGAGGGGCTCGCATCTCTCCTTCACGCGC  
CCGCCGCCCTACCTGAGGCCGCCATCCACGCCGGTTGAGTCGCGTTCTGCCGCCTCC  
CGCCTGTGGTGCCTCCTGA**ACTGCGTCCGCCGTCTAGGTAAGTTTAAAGCTCAGGTC**  
GAGACCGGGCCTTTGTCCGGCGCTCCCTTGGAGCCTACCTAGACTCAGCCGGCTCTC  
CACGCTTTGCCTGACCCTGCTTGCTCAACTCTACGTCTTTGTTTCGTTTTCTGTTCTGC  
GCCGTTACAGATCCAAGCTGTGACCGGGCGCCTACTCTAGAGCTAGCGAATTCGAATG  
GCC**ATGGCCTTACCAGTGACCGCCTTGCTCCTGCCGCTGGCCTTGCTGCTCCACGCC**  
**GCCAGGCCGGACATCCAGATGACACAGACTACATCCTCCCTGTCTGCCTCTCTGGGA**

GACAGAGTCACCATCAGTTGCAGGGCAAGTCAGGACATTAGTAAATATTTAAATTG  
GTATCAGCAGAAACCAGATGGAACGTAAACTCCTGATCTACCATACATCAAGATT  
ACACTCAGGAGTCCCATCAAGGTTCAAGTGGCAGTGGGTCTGGAACAGATTATTCTCT  
CACCATTAGCAACCTGGAGCAAGAAGATATTGCCACTTACTTTTGCCAACAGGGTAA  
TACGCTTCCGTACACGTTTCGGAGGGGGGACTAAGTTGGAAATAACACGGGCTGATG  
CTGCACCAACTGTATCCATCTTCCCACCATCCAGTAATGGTGGCGGTGGCTCGGGCG  
GTGGTGGGTCGGGTGGCGGCGGATCTGAGGTGAAACTGCAGGAGTCAGGACCTGGC  
CTGGTGGCGCCCTCACAGAGCCTGTCCGTCACATGCACTGTCTCAGGGGTCTCATT  
CCCGACTATGGTGTAAGCTGGATTCGCCAGCCTCCACGAAAGGGTCTGGAGTGGCTG  
GGAGTAATATGGGGTAGTGAAACCACATACTATAATTCAGCTCTCAAATCCAGACTG  
ACCATCATCAAGGACAACCTCAAGAGCCAAGTTTTCTTAAAAATGAACAGTCTGCA  
AACTGATGACACAGCCATTTACTACTGTGCCAAACATTATTACTACGGTGGTAGCTA  
TGCTATGGACTACTGGGGTCAAGGAACCTCAGTCACCGTCTCCTCAGGTGGAGGCGG  
GTCTGGGGGCGGAGGTTTCAGGCGGGGGTGGTTCCGAGCCCAAATCTCCTGACAAAA  
CTCACACATGCCATTTTGGGTGCTGGTGGTGGTGGTGGAGTCTGGCTTGCTATA  
GCTTGCTAGTAACAGTGGCCTTTATTATTTTCTGGGTGAAACGGGGCAGAAAGAAAC  
TCCTGTATATATTCAAACAACCATTTATGAGACCAGTACAAACTACTCAAGAGGAAG  
ATGGCTGTAGCTGCCGATTTCCAGAAGAAGAAGAAGGAGGATGTGAACTGAGAGTG  
AAGTTCAGCAGGAGCGCAGACGCCCCCGGTACCAGCAGGGCCAGAACCAGCTCTA  
TAACGAGCTCAATCTAGGACGAAGAGAGGAGTACGATGTTTTGGACAAGAGACGTG  
GCCGGGACCCTGAGATGGGGGGAAAGCCGAGAAGGAAGAACCCTCAGGAAGGCCT  
GTACAATGAACTGCAGAAAGATAAGATGGCGGAGGCCTACAGTGAGATTGGGATGA  
AAGGCGAGCGCCGGAGGGGCAAGGGGCACGATGGCCTTTACCAGGGTCTCAGTACA  
GCCACCAAGGACACCTACGACGCCCTTCACATGCAGGCCCTGCCCCCTCGCTAAGTC  
GACAATCAACCTCTGGATTACAAAATTTGTGAAAGATTGACTGGTATTCTTAACTAT  
GTTGCTCCTTTTACGCTATGTGGATACGCTGCTTTAATGCCTTTGTATCATGCGTTAA  
CTAAACTTGTTTATTGCAGCTTATAATGGTTACAAATAAAGCAATAGCATCACAAAT  
TTCACAAATAAAGCATTTTTTTCTACTGCATTCTAGTTGTGGTTTGTCCAAACTCATCA  
ATGTATCTTATCATGTCTGGAATTGACTCAAATGATGTCAATTAGTCTATCAGAAGC  
TCATCTGGTCTCCCTTCCGGGGGACAAGACATCCCTGTTTAATATTTAAACAGCAGT  
GTTCCCAAACCTGGGTTCTTATATCCCTTGCTCTGGTCAACCAGGTTGCAGGGTTTCCT  
GTCCTCACAGGAACGAAGTCCCTAAAGAAACAGTGGCAGCCAGGTTTAGCCCCGGA  
ATTGACTGGATTCCCTTTTTTAGGGCCCATTTGGTATGGCTTTTTCCCCGTATCCCCCA  
GGTGTCTGCAGGCTCAAAGAGCAGCGAGAAGCGTTCAGAGGAAAGCGATCCCGTGC  
CACCTTCCCCGTGCCCGGGCTGTCCCCGCACGCTGCCGGCTCGGGGATGCGGGGGG  
AGCGCCGACCAGGAGCGGAGCCCCGGGCGGCTCGCTGCTGCCCCCTAGCGGGGGAG  
GGACGTAATTACATCCCTGGGGGCTTTGGGGGGGGGCTGTCCCTGATATCTATAACA  
AGAAAATATATATAATAAGTTATCACGTAAGTAGAACATGAAATAACAATATAA  
TTATCGTATGAGTTAAATCTTAAAAGTCACGTAAGATAATCATGCGTCATTTTGA  
CTCACGCGGTCGTTATAGTTCAAATCAGTGACACTTACCGCATTGACAAGCACGCC  
TCACGGGAGCTCCAAGCGGCGACTGAGATGTCCTAAATGCACAGCGACGGATTTCG  
GCTATTTAGAAAAGAGAGCAATATTTCAAGAATGCATGCGTCAATTTTACGCAG  
ACTATCTTTCTAGGGTTAATCTAGCTGCATCAGGATCATATCGTCCGGTCTTTTTTC  
CGGCTCAGTCATCGCCCAAGCTGGCGCTATCTGGGCATCGGGGAGGAAGAAGCCCG  
TGCCTTTTCCCGCGAGGTTGAAGCGGCATGGAAAGAGTTTGCCGAGGATGACTGCTG  
CTGCATTGACGTTGAGCGAAAACGCACGTTTACCATGATGATTCGGGAAGGTGTGGC

CATGCACGCCTTTAACGGTGAACGTTCGTTTCAGGCCACCTGGGATAACCAGTTCGTC  
GCGGCTTTTCCGGACACAGTTCGGGATGGTCAGCCCGAAGCGCATCAGCAACCCGA  
ACAATACCGGCGACAGCCGGAAGTCCCGTGCCGGTGTGCAGATTAATGACAGCGGT  
GCGGGCGCTGGGATATTACGTCAGCGAGGACGGGTATCCTGGCTGGATGCCGCAGAA  
ATGGACATGGATACCCCGTGAGTTACCCGGCGGGCGCGCGCCCTGCAAAGTAAACT  
GGATGGCTTTCTTGCCGCCAAGGATCTGATGGCGCAGGGGATCAAGCTCTGATCAAG  
AGACAGGATGAGGATCGTTTCGCATGATTGAACAAGATGGATTGCACGCAGGTTCT  
CCGGCCGCTTGGGTGGAGAGGCTATTCGGCTATGACTGGGCACAACAGACAATCGG  
CTGCTCTGATGCCGCCGTGTTCCGGCTGTCAGCGCAGGGGGCGCCCGGTTCTTTTTGTC  
AAGACCGACCTGTCCGGTGCCCTGAATGAACTGCAAGACGAGGCAGCGCGGCTATC  
GTGGCTGGCCACGACGGGCGTTCCTTGCGCAGCTGTGCTCGACGTTGTCACTGAAGC  
GGAAAGGGACTGGCTGCTATTGGGGCAAGTGCCGGGGCAGGATCTCCTGTCATCTC  
ACCTTGCTCCTGCCGAGAAAGTATCCATCATGGCTGATGCAATGCGGCGGCTGCATA  
CGCTTGATCCGGCTACCTGCCATTTCGACCACCAAGCGAAACATCGCATCGAGCGA  
GCACGTAATCGGATGGAAGCCGGTCTTGTCGATCAGGATGATCTGGACGAAGAGCA  
TCAGGGGCTCGCGCCAGCCGAACTGTTCCGCCAGGCTCAAGGCGAGCATGCCCGACG  
GCGAGGATCTCGTCGTGACCCATGGCGATGCCTGCTTGCCGAATATCATGGTGGAAA  
ATGGCCGCTTTTCTGGATTCATCGACTGTGGCCGGCTGGGTGTGGCGGACCGCTATC  
AGGACATAGCGTTGGCTACCCGTGATATTGCTGAAGAGCTTGGCGGCGAATGGGCT  
GACCGCTTCCTCGTGCTTTACGGTATCGCCGCTCCCGATTTCGACGCGCATCGCCTTCT  
ATCGCCTTCTTGACGAGTTCTTCTGAATTATTAACGCTTACAATTTCTGATGCGGTA  
TTTTCTCCTTACGCATCTGTGCGGTATTTACACCCGCATCAGGTGGCACTTTTCCGGG  
AAATGTGCGCGGAACCCCTATTTGTTTATTTTTCTAAATACATTCAAATATGTATCCG  
CTCATGAGACAATAACCCTGATAAATGCTTCAATAATAGCACGTGCTAAAACCTTCAT  
TTTTAATTTAAAAGGATCTAGGTGAAGATCCTTTTTGATAATCTCATGACCAAAAATC  
CCTAACGTGAGTTTTTCGTTCCACTGAGCGTCAGACCCCGTAGAAAAGATCAAAGGA  
TCTTCTTGAGATCCTTTTTTTCTGCGCGTAATCTGCTGCTTGCAAACAAAAAACAC  
CGCTACCAGCGGTGGTTTGTGTTGCCGGATCAAGAGCTACCAACTCTTTTCCGAAGG  
TAACTGGCTTCAGCAGAGCGCAGATAACCAAATACTGTTCTTCTAGTGTAGCCGTAGT  
TAGGCCACCACTTCAAGAACTCTGTAGCACCGCCTACATACCTCGCTCTGCTAATCC  
TGTTACCAGTGGCTGCTGCCAGTGGCGATAAGTCGTGTCTTACCGGGTTGGACTCAA  
GACGATAGTTACCGGATAAGGCGCAGCGGTCCGGCTGAACGGGGGGTTCGTGCACA  
CAGCCCAGCTTGAGCGAACGACCTACACCGAACTGAGATACCTACAGCGTGAGCT  
ATGAGAAAGCGCCACGCTTCCCGAAGGGAGAAAGGCGGACAGGTATCCGGTAAGC  
GGCAGGGTTCGGAACAGGAGAGCGCACGAGGGAGCTTCCAGGGGGAAACGCCTGGT  
ATCTTTATAGTCTGTGCGGTTTCGCCACCTCTGACTTGAGCGTCGATTTTTGTGATG  
CTCGTCAGGGGGGCGGAGCCTATGGAAAAACGCCAGCAACGCGGCCTTTTTACGGT  
TCCTGGCCTTTTGCTGGCCTTTTGCTCACATGTTCTT

### ***Detailed CAR T-cell Production Protocol***

This study was conducted in accordance with the Declaration of Helsinki. Donor peripheral blood mononuclear cells (PBMCs) were isolated from whole blood by Ficoll gradient centrifugation and rested in AIM-V (Thermo-Fisher) for 2-24 hours. Rested cells were washed in phosphate buffered saline and suspended in Neon Resuspension Buffer T at a concentration of  $4 \times 10^7$ /ml with 20 ug/ml piggyBac transposase mRNA and 50 ug/ml of the CAR transposon plasmid. Up to  $50 \times 10^7$  cells were electroporated in 100ul aliquots using the Neon transfection system (Thermo-Fisher) with 1 pulse at 2400v for 20ms. Transduced cells were rested in media overnight, harvested, counted, suspended in AIM-V supplemented with 10% autologous serum (complete AIM-V) at  $1 \times 10^6$ /ml and transferred to a G-Rex10 culture flask (Wilson Wolf Manufacturing). Irradiated (30 Gy) donor PBMC feeder cells were added at an effector:feeder ratio of 1:2 and supplemented with interleukin-15 at a final concentration of 200 IU/ml. Interleukin-15 was replenished every 2-3 days and irradiated PBMCs every 7 days. CAR T cell manufacturing was completed within 15 days of electroporation for both products, and products were cryopreserved at  $1 \times 10^7$  cells/ml in 70% saline (Baxter), 20% Albumex20 (CSL Behring) and 10% dimethyl sulfoxide (WAK-Chemie Medical).

### ***Flow cytometry detection of CAR T-cells***

Cells were extracted from biopsy specimens using the Miltenyi gentleMACS Dissociator (Miltenyi Biotec, Bergisch Gladbach, Germany). Mononuclear cells were isolated from the peripheral blood and ascites by ficoll gradient centrifugation. Live cells were identified by exclusion of 7AAD (eBioscience, Thermo Fisher) and stained using fluorophore conjugated antibodies (BD Biosciences Franklin Lakes, NJ, Table S1). The FMC63-specific anti-idiotypic

antibody (a gift from Prof Laurence Cooper, MD Anderson<sup>19</sup>) was conjugated using the Alexa Fluor 647 labelling kit (Invitrogen, Thermo Fisher Scientific, Waltham, MA).

Immunophenotypic analysis of malignant CAR T-cells was performed on FACS Canto or Fortessa flow cytometers (BD Biosciences) and analyzed using FCS Express 6 (De Novo Software, Pasadena, CA).

### *Abseq immunophenotypic analysis*

Aliquots of one million cells were incubated with human Fc Block (BD Pharmingen) followed by a cocktail of antibody-oligonucleotide conjugates (AbO) (BD Biosciences) (Table S1) for 45 minutes. Malignant cells were loaded directly onto a 10X Chromium. CAR T-cell product was sorted for viable CD3<sup>+</sup>CAR19<sup>+</sup> cells on a BD FACSAria IIIu (BD Biosciences) and loaded onto a 10X Chromium platform.

Library preparation was performed using Chromium Single Cell 3' Reagents Kits v2 (10X Genomics, PN-120267) and v3 (10X Genomics, PN-1000092). An AbO-specific PCR1 primer was used to amplify the AbSeq library which were separated following cDNA amplification by SPRIselect size selection (Beckman Coulter). Sample index PCRs were performed according to manufacturers' instructions, final libraries were pooled and sequenced together on NextSeq500 or NovaSeq6000 platforms (Illumina). Library quality control was performed using a combination of agarose gel electrophoresis, Quant-iT PicoGreen (Invitrogen) and LabChip GX (Perkin Elmer).

The Cellranger pipeline was applied to obtain the protein expression (AbSeq) matrix. This resulted in a total of 3173 cells for the product and 4362 cells for the tumor sample. All plots

with AbSeq expression values show the result of a centered-log-ratio normalization applied to the raw counts.

### ***Phosphoflow***

$5 \times 10^5$  rested cells were fixed and permeabilized with PhosFlow Lyse/Fix Buffer and PhosFlow Perm Buffer III (BD Biosciences). Cells were stained with anti-CD3-APC, anti-CD4-PECy7, anti-CD8-Pacific Blue, anti-CD3zeta(pY142)-PE, anti-AKT(pS473)-AF488 and anti-ZAP70(pY319)-AF488 (BD Biosciences, Table S1). Data were collected on the LSRFortessa flow cytometer (BD Biosciences) and analyzed using FCS Express 6. To control for autofluorescence, an FMO sample was stained with surface antibodies.

### ***Flow cytometry cell sorting***

CD4<sup>+</sup>, CD8<sup>+</sup> and CAR<sup>+</sup> T-cells were selected from healthy donor peripheral blood, the patient's CAR T-cell product, enriched peripheral blood CAR T-cells and malignant CAR T-cell tumor by flow cytometry sorting on the FACSAria III sorter (BD Biosciences). Untransduced T-cells from the peripheral blood of healthy donors were identified as lineage negative (CD19<sup>neg</sup>, CD56<sup>neg</sup>, CD14<sup>neg</sup>) and CD4<sup>+</sup> or CD8<sup>+</sup>. CAR<sup>+</sup> T-cells were identified as CD4<sup>+</sup>CAR<sup>+</sup> or CD8<sup>+</sup>CAR<sup>+</sup>.



**Table S1- Abseq and fluorophore conjugated antibodies used for phenotypic analysis, phosphoflow and flow cytometry sorting- all from BD Bioscience**

Target	Clone	Barcode ID (precommercial in brackets)	Catalogue number
<b>CD127</b>	HIL-7R-M21	AHS0028	940012
<b>CD14</b>	MφP9	AHS0037	940005
<b>CD161</b>	DX12	AHS0002	940070
<b>CD183</b>	1C6/CXCR3	AHS0031	940030
<b>CD185 (CXCR5)</b>	RF8B2	AHS0039	940042
<b>CD19</b>	HIB19	(v2a_Hs_0030)	
<b>CD194</b>	1G1	AHS0038	940047
<b>CD196 (CCR6)</b>	11A9	AHS0034	940033
<b>CD197 (CCR7)</b>	150503	(v2a_Hs_007)	
<b>CD25</b>	M-A251	(v2a_Hs_0026)	
<b>CD27</b>	M-T271	AHS0025	940018
<b>CD28</b>	CD28.2	AHS0024	940017
<b>CD3</b>	SK7	AHS0033	940000
<b>CD38</b>	HIT2	AHS0022	940013
<b>CD4</b>	SK3	AHS0032	940001
<b>CD45RA</b>	HI100	AHS0009 (v2a_Hs_0029)	940011
<b>CD45RO</b>	UCHL1	AHS0036	940022
<b>CD8</b>	RPA-T8	AHS0027	940003
<b>CD95</b>	DX2	AHS0023	940037
<b>HLA-DR</b>	G46-6	(v2a_Hs_0035)	
<b>PD1 (CD279)</b>	MIH4	(v2a_Hs_0014)	
<b>CD10</b>	HI10a	AHS0051	940045
<b>CD11b</b>	M1/70	AHS0005	940008
<b>CD11c</b>	B-ly6	AHS0056	940024
<b>CD137</b>	4B4-1	AHS0003	940055
<b>CD141</b>	1A4	AHS0083	940079
<b>CD154</b>	TRAP1	AHS0077	940053
<b>CD16</b>	3G8	AHS0053	940006
<b>CD20</b>	2H7	AHS0008	940016
<b>CD206</b>	19.2	AHS0072	940068
<b>CD21</b>	B-ly4	AHS0074	940048
<b>CD274 (B7-H1)</b>	MIH1	AHS0004	940035
<b>CD40</b>	5C3	AHS0117	940049
<b>CD56</b>	NCAM16.2	AHS0019	940007
<b>CD80 (B7-1)</b>	L307.4	AHS0046	
<b>CD86 (B7-2)</b>	2331 (FUN-1)	AHS0057	940025
<b>IgD</b>	IA6-2	AHS0058	940026

<b>IgG</b>	G18-145	AHS0059	940027
<b>LAG-3 (CD223)</b>	T47-530	AHS0018	940080
<b>TIM-3 (CD366)</b>	7D3	AHS0016	940066
<b>CD19</b>	SJ25C1	AHS0030	940004
<b>CD25</b>	2A3	AHS0026	940009
<b>CD197 (CCR7)</b>	3D12	AHS0007	940014
<b>PD1 (CD279)</b>	EH12.1	AHS0014	940015
<b>Target</b>	<b>Clone</b>	<b>Fluorophore</b>	<b>Catalogue number</b>
<b>CD2</b>	RPA-2.10	FITC	555326
<b>CD3</b>	UCHT1	BV480	566105
<b>CD3</b>	UCHT1	Pacific Blue	558117
<b>CD3</b>	UCHT1	BV510	563109
<b>CD3</b>	SK7	PECy7	341091
<b>CD4</b>	SK3	APC	340443
<b>CD4</b>	SK3	PE-Cy7	557852
<b>CD4</b>	RPA-T4	BUV395	564724
<b>CD8</b>	RPA-T8	APC-R700	565165
<b>CD8</b>	RPA-T8	Pacific Blue	558207
<b>CD8</b>	SK1	FITC	347313
<b>CD8</b>	SK1	PE	340046
<b>CD14</b>	M5E2	PE-Cy7	557742
<b>CD19</b>	4G7	PerCP	347544
<b>CD19</b>	HIB19	PE-Cy5	555414
<b>CD56</b>	NCAM16.2	FITC	340410
<b>CD3<math>\zeta</math>-pY142</b>	K25-407.69	PE	558448
<b>ZAP70-pY319</b>	17A/P-ZAP70	AF488	557818
<b>SRC-pY418</b>	K98-37	PE	560094
<b>Akt-pS473</b>	M89-61	AF488	560404

### ***T-Cell receptor clonality analysis***

Multiplex PCR was performed using BIOMED-2 primers targeting the V and J regions of the T-cell receptor gamma (TCRG) with the Invivoscribe Identiclone TCRG Gene Clonality Assay, followed by fragment analysis by capillary electrophoresis.

T-cell receptor beta (TRB) loci deep amplicon sequencing was performed using LymphoTrack TRB (Invivoscribe, San Diego, CA). Sequence assembly from FASTQs, annotation and error

correction was performed by MiXCR<sup>20</sup> with diversity assessment, VDJ family usage analysis performed using VDJtools (ver 1.1.9).<sup>21</sup>

### ***Hybridization-based next generation sequencing analysis***

Extracted DNA was analysed for the presence of mutations in a panel of genes commonly mutated in haematological malignancies as previously described.<sup>22</sup> Indexed libraries were sequenced on an Illumina NextSeq (paired-end 75 bp reads). After base calling and de-multiplexing, a Seqliner-framework analysis pipeline was used to align reads to the human reference genome (GRCh37 assembly) using BWA-MEM, followed by marking of duplicate reads, base quality score recalibration, local indel realignment and variant calling using GATK Haplotype Caller (<https://software.broadinstitute.org/gatk/>). Aligned sequence data was processed through a dedicated bioinformatics pipeline which included variant calling with GATK4/Mutect2 (<https://software.broadinstitute.org/gatk/>) in order to improve detection of low level acquired variants. Genomic copy number analysis was performed using on and off target reads from this hybridization-based NGS panel.<sup>22,23</sup>

### ***Transgene copy number analysis***

Droplet digital PCR was conducted on genomic DNA<sup>22</sup> using a custom Bio-Rad PrimerPCR ddPCR primer/probe specific for the CAR gene at the junction of CD28 transmembrane and 4-1BB intracellular sequences and the Bio-Rad Human RPP30. Copy number assay primer/probe (Bio-Rad, Hercules, CA) CAR and RPP30 gene copies per microliter were absolutely quantified utilising QuantaSoft Software v1.7.4 (Bio-Rad).

CAR copies per cell (CCPC) were calculated using the equation:

CCPC = 2 x (CAR copies/ul)/(RPP30 copies/ul)

### ***Whole genome sequencing analysis***

Sequencing libraries were prepared from 100 ng of genomic DNA using the NEBNext Ultra II DNA Library Prep Kit for Illumina (New England Biolabs, Ipswich, MA, USA) with a double-sided SPRI bead size selection and 6 cycles of PCR. Whole genome sequencing was performed by the Australian Genome Research Facility (AGRF) on the NovaSeq 6000 platform (Illumina, San Diego CA, USA) with a 2 × 150 bp read length using NovaSeq S4 300-cycle reagent kit. Each sample was sequenced to a minimum of 30-fold base coverage (30X) per sample with a total output of a minimum 100GB. Primary data analysis was performed in real time by the NovaSeq Control Software v1.6.0 and Real Time Analysis (RTA) v3.4.4. Demultiplexed fastq files were generated using Illumina's bcl2fastq software (version 2.20.0.422).

A modified human reference was generated by concatenating GRCh38 with the CAR19 sequence as an additional contig. Reads were aligned to the modified reference using Sentieon<sup>24</sup> with default settings. Structural Variants (SVs) were called using the SURVIVOR pipeline<sup>25,26</sup>. Alignments were processed through Individual SV callers Delly (v0.8.2)<sup>27</sup>, Lumpy (v0.2.13)<sup>28</sup>, and Manta (v1.6.0)<sup>29</sup>. The consensus among these callers was determined by SURVIVOR (v1.0.7) using the parameters "1000 2 1 0 0". Reads with low mapping quality (MQ < 4 per sample) were identified using samtools view and samtools depth and then clustered together using SURVIVOR "bincov" with parameters 10 (window size) and 2 (minimum number of reads). SVs per sample were filtered using SURVIVOR "filter" to obtain SV calls outside of hard to map regions. The SV across the samples were merged using SURVIVOR "merge" with parameters "1000 1 1 0 0 0" to form the final multi-sample VCF file. The retained SVs were

annotated with `annotatePeaks.pl` from HOMER<sup>30</sup> using the hg38 build. CAR19 insertions in the malignancy detected by mu insertion analysis were confirmed by searching alignment files for paired end split reads between the CAR19 “contig” and regions of the autosomes, excluding calls that did not indicate a full-length insertion of CAR19.

### ***Whole transcriptome analysis***

Low input RNA-seq libraries were prepared using the SMARTer Stranded Total RNA-Seq kit v2 - Pico input mammalian (Takara Bio USA, Inc, CA) by AGRF and sequenced at 1 × 100 bp SE on an Illumina Novaseq 6000 SP 100 lane.

Library sequencing quality was determined using FastQC and FastQ0 Screen, Illumina adaptor sequence and reads of < 20 base pairs were trimmed using Trim Galore!

(BabrahamBioinformatics: [www.bioinformatics.babraham.ac.uk/](http://www.bioinformatics.babraham.ac.uk/)). Reads were aligned to a custom genome (hg38 and CART-insert) using STAR<sup>30</sup> with Refseq annotations as a guide. Read counts data corresponding to Refseq transcript annotations were generated using HTSeq.<sup>31</sup> Alignments and transcriptional shadows were visualised using IGV (v2.72).<sup>32</sup> Genome position analyses were performed using genomic ranges<sup>33</sup> based on RefSeq annotations imported with ‘`rtracklayer`’<sup>34</sup> and gene lists were annotated with KEGG pathways (adjusted p value <0.05) using the `clusterProfiler` package.<sup>35</sup>

All analyses were performed in the R Statistical Environment (<http://www.Rproject.org>) with `tidyverse`.<sup>36</sup> Counts data were background corrected and normalized for library size using `edgeR`<sup>37</sup> then transformed using `voom`<sup>38</sup> for differential expression analysis using LIMMA<sup>39</sup> (4-fold change, `sdj.p` <0.01).

### ***In silico analysis of transcriptional readthrough mediated gene expression***

In silico impact was estimated for genic insertion sites using RefSeq gene annotations. Briefly, where exons within a transcriptional shadow appeared overexpressed, if all coding exons were downstream, the ORF was considered intact and the proportion of reads arising due to insertion was estimated by taking the ratio of spliced reads relative to the proportion of spliced reads to the exon coverage. If insertion was within the coding region, the resultant sequence was verified for loss of frame using in silico translation and comparison to wildtype transcript sequence.

Contribution of insertion to total gene signal was estimated as above.

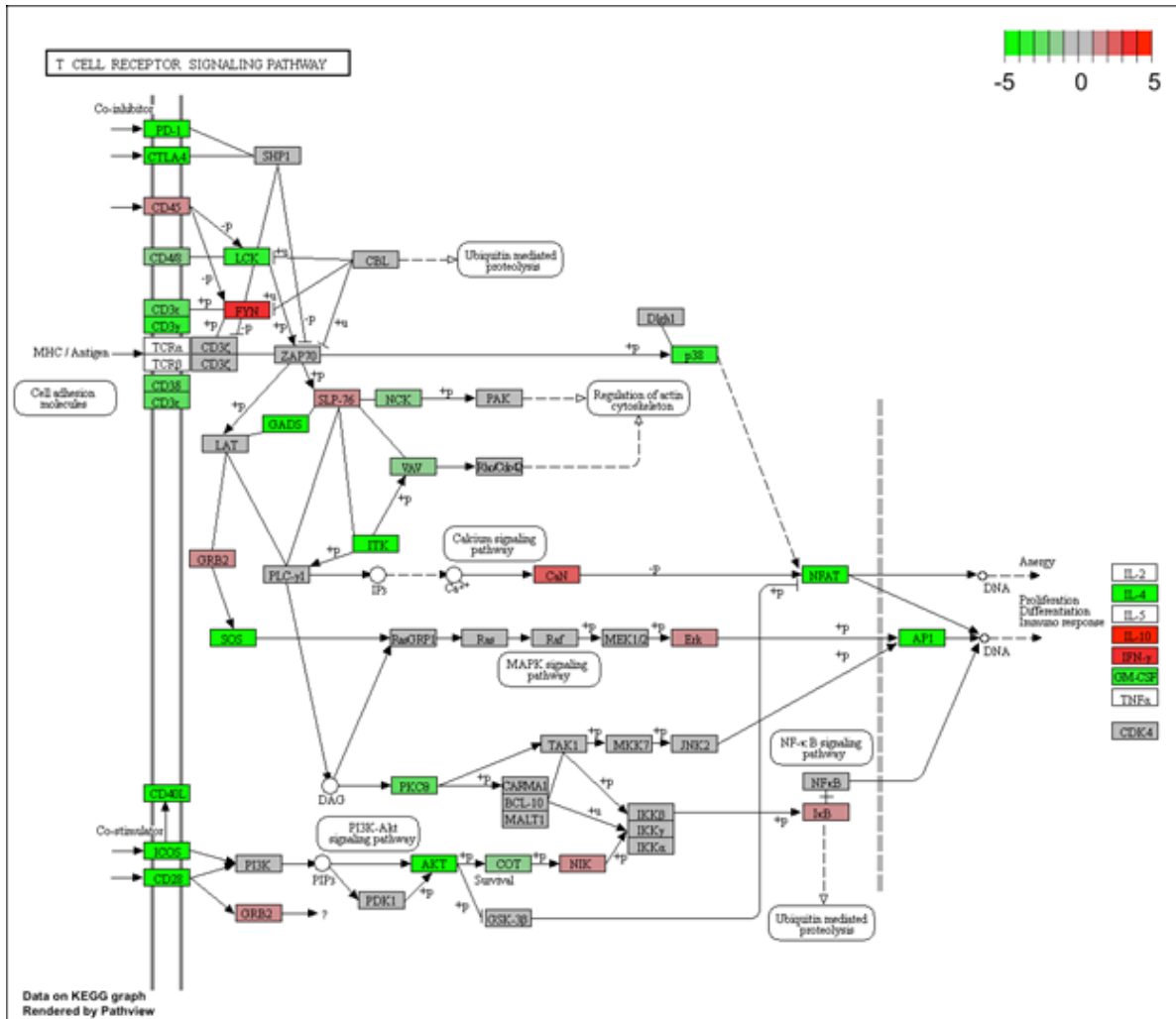


**Figure S3. FYN and T-cell receptor activation pathways.** KEGG pathway showing predominantly reduced levels of T-cell receptor associated genes and upregulation of FYN in the malignant CAR T-cells compared to untransduced healthy donor controls (green= down-regulated, red=up-regulated).

**Table S2. Integration sites within the malignant CAR T-cells and their effect on expression of surrounding genes in Patient 8**

Chr	INSERT MAPPING			GENOMIC CONTEXT AND RNA SEQ		
	Insert Site	Strand	Transcriptional shadow (kbp)	Gene same strand within shadow	Observed Log2FC (MalignancyCPM vs ProductCPM)	<i>in silico</i> evidence of functional product
chr1	8,3508,456	+	100	Non-coding RNA LOC107985043		Possible increase of uncertain significance
chr6	90,105,820	-	150	BACH2	-0.71	No
chr6	142,807,281	+	100			No
ChrX	65746639	-	30			No



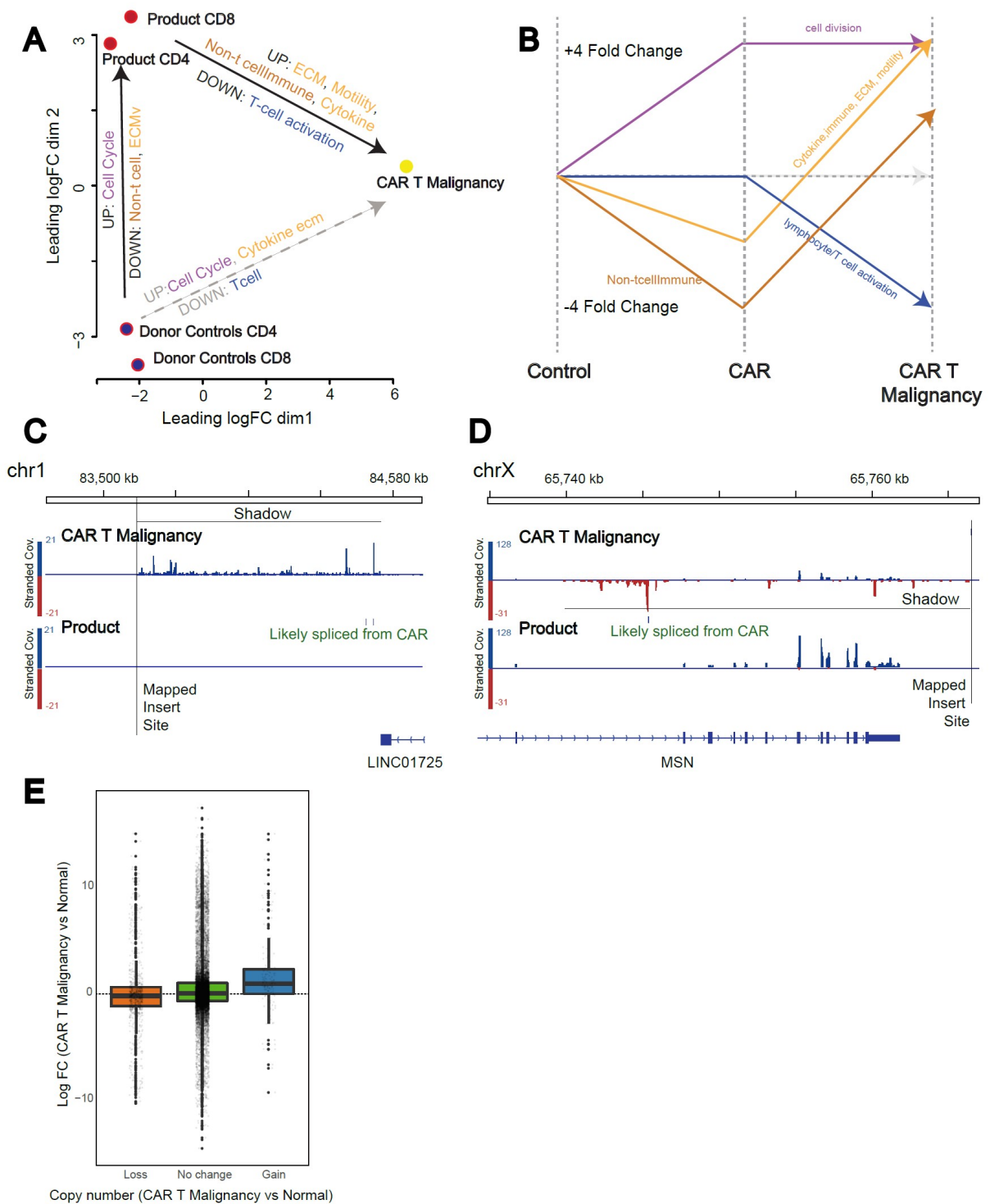


**Figure S4. Transcription Analysis of Malignant CAR T-cells Compared to Non-Malignant CAR<sup>+</sup> and Untransduced T-cells related to Patient 8.** (A) Multidimensional scaling of global

gene expression from malignant CAR T-cells (Malignancy), non-malignant CD4<sup>+</sup> and CD8<sup>+</sup> CAR T-cells from the product (Product) and untransduced healthy donor CD4<sup>+</sup> and CD8<sup>+</sup> T-cells (Donor Controls). (B) Line drawing showing 4-fold differential expression of clusters of genes in the malignant CAR T-cells (Malignancy) compared to CD8<sup>+</sup> T-cells from the CAR T-cell product (CAR) and untransduced related healthy donor T-cells (Control). (C) Example of transcriptional readthrough/shadow seen in the malignant CAR T-cells at the point of insertion proximal to the non-coding mRNA LOC107985043 producing increased positive strand expression (D) transcriptional readthrough at the point of insertion inverse to the MSN3 gene showing no increase in exonic expression. (E) Correlation between copy number variation and altered gene expression showing correlation between copy number gain and increased gene expression (blue box) in the malignant CAR T-cells (Malignancy) compared to CAR<sup>+</sup>CD8<sup>+</sup> T-cells isolated from the product.

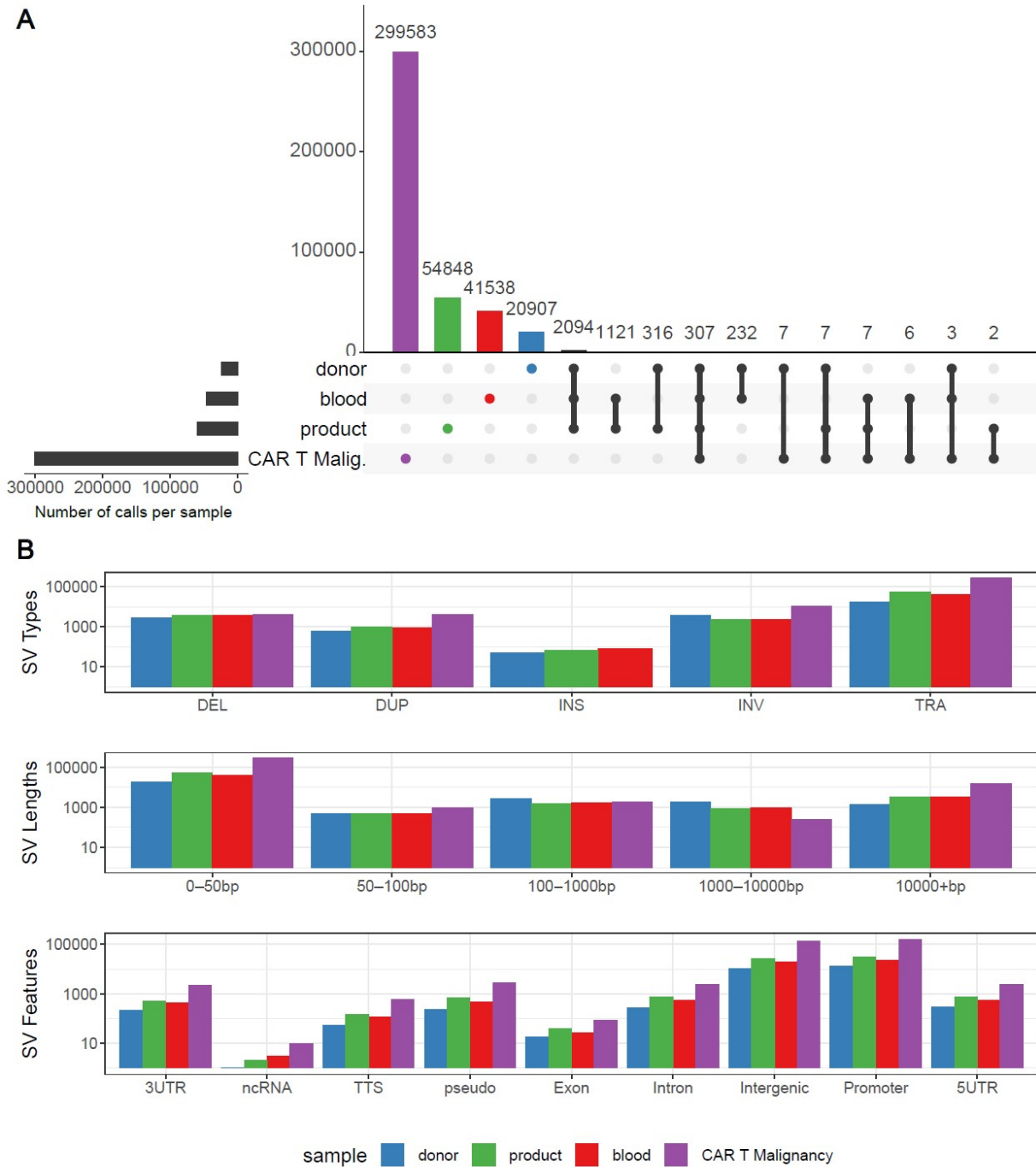


**Figure S5. Structural variants across whole genome sequenced samples related to Patient 8.**

(A) UpSet plot showing the intersection of structural variants (SV) calls across DNA extracted from CD8<sup>+</sup> T-cells isolated from untransduced healthy donor T-cells (donor), CD8<sup>+</sup> CAR T-cells from the CAR T-cell product (product), expanded from Patient 8's peripheral blood (blood) and

from the malignancy (CAR T Malignancy). SVs detected uniquely within each sample are shaded in colors, maintained throughout the figure. On the bottom left is the number of calls per sample; intersections between samples (black) are shown by connecting bars in lower right plot.

(B) Distribution of SVs called uniquely for each sample, including SV type (DEL=deletions; DUP=duplications; INS=insertions; INV=inversions; TRA=translocations; 3UTR= 3' untranslated regions; ncRNA= non-coding RNA; TTS= triplex target DNA sites; pseudo= pseudogenes; 5UTR= 5' untranslated region), the length of each SV, and the genomic annotation per SV.

## REFERENCES

1. Uetsuki T, Naito A, Nagata S, Kaziro Y. Isolation and characterization of the human chromosomal gene for polypeptide chain elongation factor-1 alpha. *J Biol Chem.* 1989;264(10):5791-5798.
2. Kim DW, Uetsuki T, Kaziro Y, Yamaguchi N, Sugano S. Use of the human elongation factor 1 alpha promoter as a versatile and efficient expression system. *Gene.* 1990;91(2):217-223.
3. Sweet BH, Hilleman MR. The vacuolating virus, S.V. 40. *Proc Soc Exp Biol Med.* 1960;105:420-427.
4. Fiers W, Contreras R, Haegemann G, et al. Complete nucleotide sequence of SV40 DNA. *Nature.* 1978;273(5658):113-120.
5. Hansen J, Mailand E, Swaminathan KK, Schreiber J, Angelici B, Benenson Y. Transplantation of prokaryotic two-component signaling pathways into mammalian cells. *Proc Natl Acad Sci U S A.* 2014;111(44):15705-15710.
6. Ramezani A, Hawley TS, Hawley RG. Performance- and safety-enhanced lentiviral vectors containing the human interferon-beta scaffold attachment region and the chicken beta-globin insulator. *Blood.* 2003;101(12):4717-4724.
7. Emery DW, Yannaki E, Tubb J, Nishino T, Li Q, Stamatoyannopoulos G. Development of virus vectors for gene therapy of beta chain hemoglobinopathies: flanking with a chromatin insulator reduces gamma-globin gene silencing in vivo. *Blood.* 2002;100(6):2012-2019.
8. Rivella S, Callegari JA, May C, Tan CW, Sadelain M. The cHS4 insulator increases the probability of retroviral expression at random chromosomal integration sites. *J Virol.* 2000;74(10):4679-4687.
9. Sharma N, Hollensen AK, Bak RO, Staunstrup NH, Schroder LD, Mikkelsen JG. The impact of cHS4 insulators on DNA transposon vector mobilization and silencing in retinal pigment epithelium cells. *PLoS One.* 2012;7(10):e48421.
10. Cary LC, Goebel M, Corsaro BG, Wang HG, Rosen E, Fraser MJ. Transposon mutagenesis of baculoviruses: analysis of *Trichoplusia ni* transposon IFP2 insertions within the FP-locus of nuclear polyhedrosis viruses. *Virology.* 1989;172(1):156-169.
11. Fraser MJ, Cary L, Boonvisudhi K, Wang HG. Assay for movement of Lepidopteran transposon IFP2 in insect cells using a baculovirus genome as a target DNA. *Virology.* 1995;211(2):397-407.
12. Fraser MJ, Ciszczon T, Elick T, Bauser C. Precise excision of TTAA-specific lepidopteran transposons piggyBac (IFP2) and tagalong (TFP3) from the baculovirus genome in cell lines from two species of Lepidoptera. *Insect Mol Biol.* 1996;5(2):141-151.
13. Gohl DM, Silies MA, Gao XJ, et al. A versatile in vivo system for directed dissection of gene expression patterns. *Nat Methods.* 2011;8(3):231-237.
14. Schuldiner O, Berdnik D, Levy JM, et al. piggyBac-based mosaic screen identifies a postmitotic function for cohesin in regulating developmental axon pruning. *Dev Cell.* 2008;14(2):227-238.
15. Zola H, MacArdle PJ, Bradford T, Weedon H, Yasui H, Kurosawa Y. Preparation and characterization of a chimeric CD19 monoclonal antibody. *Immunol Cell Biol.* 1991;69 ( Pt 6):411-422.
16. Nicholson IC, Lenton KA, Little DJ, et al. Construction and characterisation of a functional CD19 specific single chain Fv fragment for immunotherapy of B lineage leukaemia and lymphoma. *Mol Immunol.* 1997;34(16-17):1157-1165.
17. Huston JS, Levinson D, Mudgett-Hunter M, et al. Protein engineering of antibody binding sites: recovery of specific activity in an anti-digoxin single-chain Fv analogue produced in *Escherichia coli*. *Proc Natl Acad Sci U S A.* 1988;85(16):5879-5883.
18. Krebber A, Bornhauser S, Burmester J, et al. Reliable cloning of functional antibody variable domains from hybridomas and spleen cell repertoires employing a reengineered phage display system. *J Immunol Methods.* 1997;201(1):35-55.
19. Jena B, Maiti S, Huls H, et al. Chimeric antigen receptor (CAR)-specific monoclonal antibody to detect CD19-specific T cells in clinical trials. *PLoS One.* 2013;8(3):e57838.
20. Bolotin DA, Poslavsky S, Mitrophanov I, et al. MiXCR: software for comprehensive adaptive immunity profiling. *Nat Methods.* 2015;12(5):380-381.
21. Shugay M, Bagaev DV, Turchaninova MA, et al. VDJtools: Unifying Post-analysis of T Cell Receptor Repertoires. *PLoS Comput Biol.* 2015;11(11):e1004503.
22. Ryland GL, Jones K, Chin M, et al. Novel genomic findings in multiple myeloma identified through routine diagnostic sequencing. *J Clin Pathol.* 2018;71(10):895-899.

23. Markham JF, Yerneni S, Ryland GL, et al. CNspecter: a web-based tool for visualisation and clinical diagnosis of copy number variation from next generation sequencing. *Sci Rep.* 2019;9(1):6426.
24. Freed D, Aldana R, Weber JA, Edwards JS. The Sentieon Genomics Tools - A fast and accurate solution to variant calling from next-generation sequence data. *bioRxiv.* 2017.
25. Jeffares DC, Jolly C, Hoti M, et al. Transient structural variations have strong effects on quantitative traits and reproductive isolation in fission yeast. *Nat Commun.* 2017;8:14061.
26. Dennenmoser S, Sedlazeck FJ, Schatz MC, Altmuller J, Zytnicki M, Nolte AW. Genome-wide patterns of transposon proliferation in an evolutionary young hybrid fish. *Mol Ecol.* 2019;28(6):1491-1505.
27. Rausch T, Zichner T, Schlattl A, Stutz AM, Benes V, Korbel JO. DELLY: structural variant discovery by integrated paired-end and split-read analysis. *Bioinformatics.* 2012;28(18):i333-i339.
28. Layer RM, Chiang C, Quinlan AR, Hall IM. LUMPY: a probabilistic framework for structural variant discovery. *Genome Biol.* 2014;15(6):R84.
29. Chen X, Schulz-Trieglaff O, Shaw R, et al. Manta: rapid detection of structural variants and indels for germline and cancer sequencing applications. *Bioinformatics.* 2016;32(8):1220-1222.
30. Heinz S, Benner C, Spann N, et al. Simple combinations of lineage-determining transcription factors prime cis-regulatory elements required for macrophage and B cell identities. *Mol Cell.* 2010;38(4):576-589.